Precipitation Discrimination from Satellite Infrared Temperatures over the CCOPE Mesonet Region

MITCHELL WEISS

Research and Data Systems Corp., Lanham, MD 20706

ERIC A. SMITH

Department of Meteorology and Supercomputer Computations Research Institute, Florida State University, Tallahassee, FL 32306

(Manuscript received 19 December 1985; in final form 3 December 1986)

ABSTRACT

A quantitative investigation of the relationship between satellite-derived cloud-top temperature parameters and the detection of intense convective rainfall is described. The area of study is that of the Cooperative Convective Precipitation Experiment (CCOPE), which was held near Miles City, Montana during the summer of 1981. Cloud-top temperatures, derived from the GOES-West operational satellite, were used to calculate a variety of parameters for objectively quantifying the convective intensity of a storm. A dense network of raingages provided verification of surface rainfall. The cloud-top temperature field and surface rainfall data were processed into equally sized grid domains in order to best depict the individual samples of instantaneous precipitation.

The technique of statistical discriminant analysis was used to determine which combinations of cloud-top temperature parameters best classify rain versus no-rain occurrence using three different rain-rate cutoffs: 1, 4, and 10 mm h^{-1}. Time lags within the 30 min rainfall verification were tested to determine the optimum time delay associated with rainfall reaching the ground.

A total of six storm cases were used to develop and test the statistical models. Discrimination of rain events was found to be most accurate when using a 10 mm h^{-1} rain-rate cutoff. The parameters designated as coldest cloud-top temperature, the spatial mean of coldest cloud-top temperature, and change over time of mean coldest cloud-top temperature were found to be the best classifiers of rainfall in this study. Combining both a 10-min time lag (in terms of surface verification) with a 10 mm h^{-1} rain-rate threshold resulted in classifying over 60% of all rain and no-rain cases correctly.

1. Introduction

Previous research concerning the relationship between satellite measurements and rainfall has concentrated on the estimation of convective rainfall from visible and infrared satellite radiances. It has been repeatedly demonstrated that the sampling characteristics of the Geostationary Operational Environmental Satellites (GOES) can provide the necessary space and time resolution for conducting visible infrared rainfall studies.

Various investigations have shown that rainfall from convective clouds can be identified and estimated objectively based on cloud-top temperature fields derived from GOES infrared images. The techniques developed by Griffith et al. (1978), Lovejoy and Austin (1979a), Stout et al. (1979), Wylie (1979), and Griffith et al. (1981) designate the rain-producing portion of a convective cloud using a specific cloud-top temperature threshold. By quantifying the size and change over time of the colder cloud area during a storm's lifetime, the total volumetric rainfall is estimated. Scofield and Oliver (1977) and Reynolds and Smith (1978) have estimated rainfall using quantities such as tightest gradient of the cloud-top temperature field, the occurrence of overshooting tops, the coldest cloud-top temperature and the change over time of coldest cloud-top temperature. Whitney (1982) has incorporated the Laplacian of the cloud-top temperature field in rainfall estimation studies.

These physical parameters help locate areas of heavy rainfall within convective systems. The proper identification of heavier rain areas in regions of enhanced convection is important since, as shown in Fig. 1, it is intense rain events which contribute most to a storm's total volumetric rainfall. Only 25% of all rainfall occurrences are found above the 10 mm h^{-1} rain-rate threshold but they were responsible for approximately 75% of the total volumetric rainfall. In addition, Table 1 indicates that the probability of receiving a given rainfall amount varies significantly for a given period during the summer at Miles City, Montana. Since the probability of receiving significant rain becomes quite low by midsummer, it is important to detect and classify the *intense* rain events accurately.

This paper focuses on the problem of discriminating areas of intense rainfall from light and nonrain areas within convective clouds. A variety of cloud parameters calculated from the cloud-top temperature field are employed in the technique. The methodology of statistical discriminant analysis is applied to derive and test a series of statistical models consisting of the best combinations of cloud parameters correlated with rainfall. A series of experiments with different rain-rate

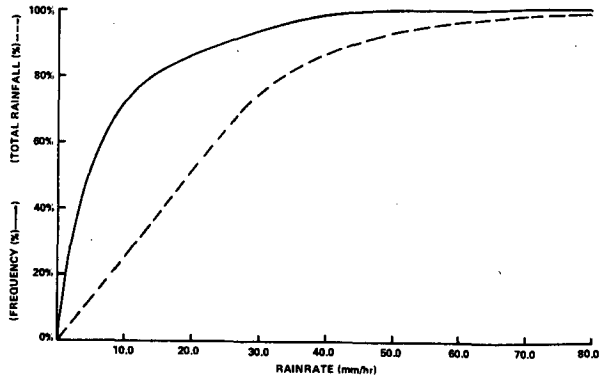

FIG. 1. Rain rate frequencies and their contribution to the total volumetric rainfall as measured from the CCOPE cases used in this study. Volumetric rainfall is defined as the total observed surface rainfall.

thresholds is conducted to seek an improved physical interpretation of the statistical method.

The data chosen for this study were collected during the Cooperative Convective Precipitation Experiment (CCOPE) field project held near Miles City, Montana in the summer of 1981. Infrared satellite data collected from the GOES-West satellite were used to calculate the cloud parameters. A dense network of surface meteorological stations located just east of Miles City were used to verify rainfall occurrence. Since many of the rain events occurred after sundown, visible channel measurements of the cloud field were not used.

2. Analysis techniques

To objectively identify higher rain-rate occurrences, these events are statistically correlated to a variety of parameters calculated from the satellite-derived cloud-top temperature field. Statistical models consisting of combinations of the most highly correlated cloud parameters are then selected to discriminate rainfall based upon a combination of different rain-rate thresholds and varying time periods of rainfall verification.

a. Cloud parameters

Before any individual cloud parameter is calculated, a threshold temperature is used to select the convective cloud area (see Wylie 1979); this step eliminates cloud sectors too warm to be considered as candidates for significant rain production. A threshold temperature of 253 K was chosen by Griffith et al. (1981) to delineate raining and nonraining convective clouds over the United States High Plains (see also Negri et al., 1984; Augustine, 1985). Wylie (1979), Scofield and Oliver (1977), and Whitney (1982) used temperature thresholds that were lower, higher, and equivalent to 253 K, respectively. Infrared pixels in the cloud-top temperature field warmer than 253 K were not included in the calculations of cloud parameters. Arkin (1979) has established a somewhat colder temperature (235 K) for estimating deep convective rainfall in tropical regions.

A description of all cloud parameters is given in Table 2. A consensus of past satellite-rainfall studies is that the coldest cloud-top temperature (CCTT) is a region of active convection and the area where rainfall is most likely to occur (e.g., Griffith et al., 1978). DelBeato and Barrell (1985) have used interpolated cloud-top temperatures derived from GMS Satellite IR image sequences to estimate rainfall in extratropical cyclones. The tightest gradient of the cloud-top temperature (GRAD) field has also been identified by Scofield and Oliver (1977) as an important signature of intense precipitation; the maximum value was shown to occur in the upwind (300-mb level) portion of the cloud, where the convection is most active and where rainfall is likely. The tightest gradient is also usually in the vicinity of the CCTT. The basic gradient equation used in this study is

$$\nabla T = \frac{\partial T}{(\partial x)} i + \frac{\partial T}{(\partial y)} j, \tag{1}$$

TABLE 1. Probability (%) of receiving accumulated rainfall totals from one week periods for Miles City, Montana (from Changnon, 1975).

	Rainfall (mm)							
Week	1.50	2.50	5.0	10.10	15.20	20.30	25.40	35.50
31 May	79	76	69	54	42	33	25	15
7 Jun	80	77	68	54	42	32	25	15
14 Jun	75	72	63	47	35	26	19	10
21 Jun	66	62	54	39	28	20	14	7
28 Jun	53	49	40	28	18	12	8	4
5 Jul	46	41	31	18	10	6	4	1
12 Jul	44	38	28	15	9	5	3	1
19 Jul	47	41	31	17	9	5	3	1
26 Jul	49	38	34	19	10	6	3	1
2 Aug	49	41	35	20	11	6	3	1
9 Aug	49	45	33	19	11	6	4	1

TABLE 2. Tabulation and description of all cloud parameters calculated from the cloud-top temperature field.

Cloud parameter subscript	Cloud parameter description	Physical relationship to rainfall
1	(CCTT) Coldest cloud-top temperature	Convectively active cloud region
2	(GRAD) Largest absolute temperature gradient	In vicinity of cloud updrafts
3	(CGRAD) Largest absolute temperature gradient of the CCTT	Cloud updrafts associated with the CCTT
4	(LAP) Largest temperature Laplacian	Cloud towers within the area of convection
5	(CLAP) Largest temperature Laplacian of the CCTT	Coldest most convective cloud towers
6	(AVGCCT) average cloud top temperature	Areal extent of the convective region
7	(CTSTT) CCTT—temperature of the tropopause	Test for overshooting tops
8	(CLAPDT) CLAP/CCTT	The physical dependency of CLAP and CGRAD to CCTT
9	(CGRADT) CGRAD/CCTT	
10	DEL − CCTT	The variability of convection and/or cloud movement over the past 30 min
11	DEL − GRAD	
12	DEL − CGRAD	
13	DEL − LAP	
14	DEL − CLAP	
15	DEL − AVGCTT	
16	DEL − CLAPDT	
17	DEL − CGRADT	

(Rows 10–17: The change over time of each respective cloud parameter)

or in absolute value, finite difference form:

$$|\nabla T| = \left| \frac{T(i-1,j) - T(i+1,j)}{(2\Delta x)} + \frac{T(i,j+1) - T(i,j-1)}{(2\Delta y)} \right| \quad (2)$$

where T is the cloud-top temperature, position (i, j) represents the mapped grid coordinate of the temperature observation over which the calculation is made, and Δx, Δy are the horizontal grid spacings. Both Δx and Δy are set sufficiently small so that the gradient measure is with respect to adjacent satellite pixels. The largest absolute temperature gradient of the CCTT (CGRAD) aided in evaluating the importance of gradients within the coldest and most highly convective cloud regions. The CGRAD was calculated only for (i, j) positions over the CCTT.

The Laplacian is potentially a powerful variable because it offers the possibility of detecting cold convective towers not associated with the CCTT (Whitney, 1982). The basic equation for the Laplacian used in this study is

$$\nabla^2 T = \frac{\partial^2 T}{(\partial x^2)} + \frac{\partial^2 T}{(\partial y^2)}, \quad (3)$$

or in finite difference form:

$$\nabla^2 T = \frac{T(i-1,j) + T(i+1,j) - 2T(i,j)}{(\Delta x)^2} + \frac{T(i,j+1) + T(i,j-1) - 2T(i,j)}{(\Delta y)^2} \quad (4)$$

where positive values of the Laplacian indicate domes of colder, more convective cloud regions and negative values indicate depressions of warmer, less convective cloud regions (see Moses, 1984, for further discussion). Analagous to CGRAD, the maximum value of the Laplacian of the CCTT (CLAP) was also utilized in the analysis.

Another cloud parameter is the average cloud-top temperature for specific cloud areas ≤253 K (AVGCCT). The Doneaud et al. (1984a, 1984b) studies explain the correlation of cloud area properties to volumetric rainfall. Other parameters include the temperature of the tropopause minus the (CTSTT), and the ratios of CLAP to CCTT (CLAPDT) and CGRAD to CCTT (CGRADT). The changes of each cloud parameter quantity over a time period of 30 min (except CTSTT) were also calculated. The change over time of CTSTT is equivalent to the change over time of CCTT.

b. Statistical models based on discriminant analysis

Discriminant analysis is a technique used to derive a statistical model from a set of independent variables which optimally discriminate between two or more groups. The technique is similar to regression analysis, except regression provides a continuous estimate of the dependent variable. In this study *rain occurrence above a threshold* takes the role of the *dependent variable* and the *cloud parameters* represent the *independent variables*. The dependent variable is coded with the value 1 to signify rain at or above the prescribed rain-rate threshold; the value 0 then signifies either no-rain or rainfall below the rain-rate threshold. Since there are a variety of uncertainties involved in establishing a continuous relationship between rain intensity and satellite measurements (see Lovejoy and Austin, 1979b), discriminate analysis is employed to minimize problems in interpreting the impact of the uncertainties.

Two computer programs in the BMDP statistical software package (Dixon et al., 1983) were used in this study to select and test these statistical models. To select the best statistical model, program BMDP-P7M was invoked. This module uses a technique called "all possible subsets regression" to generate a series of linear multiple regression equations yielding the best one parameter model, two parameter model, etc., according to set criteria. Additional information concerning this method of model selection can be found in Weisberg (1980). Since the derived models are in the form of regression equations, coefficients are derived for each cloud parameter before making quantitative estimates of the dependent variable for each rain rate threshold.

Transformation of these models to discriminate equations involves the use of a second BMDP program (BMDP-P9R). This module selects coefficients for the independent variables which best discriminate between the two groups represented by the dependent variable. From the resultant equations the numbers and percentages of samples classified correctly and incorrectly were tabulated. These percentages were then used to choose the best models for each experiment and rain-rate threshold.

c. *Experiments*

A number of experiments were designed to test the reliability of each cloud parameter in classifying surface rainfall (see Table 3). A total of three pairs of experiments were run, each pair modifying the dependent variable to account for the time lag between precipitation production and fallout. Experiments 1 and 2 classified precipitation for the 30-min period preceeding each image, while experiments 3 and 4 moved the period of verification forward by 10 min to account for conditions (discussed in Table 3) which could delay rainfall reaching the ground. Experiments 5 and 6 tested the ability of the cloud parameters to classify rainfall for the 30-min period following each image. The odd-numbered experiments required only a single surface station for verification; the even-numbered experiments required at least two surface stations for verification.

Three rain-rate thresholds were chosen: 1, 4, and 10 mm h^{-1}. The rain rate of 1 mm h^{-1} has been used by Griffith et al. (1978) as a basis for discriminating between rain and no-rain occurrence. The 4 and 10 mm h^{-1} thresholds were identified with the aid of a histogram of all 30-min rainfall measurements obtained at the surface for the 12 June, 13 July and 2 August storms. These two thresholds discriminate the three dominant regimes within the histogram itself. Although the rain rate of 10 mm h^{-1} is somewhat high for a rainfall cutoff, it is a useful threshold for classifying rain events contributing most to a cloud's total volumetric rainfall. Experiments 1–6 were run using the rain rates of 1 and 4 mm h^{-1}, but only experiments 1, 3 and 5 included the rain rates of 10 mm h^{-1}.

3. Surface and satellite data sets

The CCOPE case study days of 12 June, 13 July and the first storm event of 2 August were chosen to develop the statistical models; the days of 11 July, 1 August and the second storm event of 2 August were used as

TABLE 3. The statistical and meteorological considerations involved with modifying the time period of rainfall verification (dependent variable) for each experiment.

Experiment no.	Number of stations required to report rain	Length of time period delay	Statistical considerations	Meteorological considerations
1	1	0 Min	Delineation of rain vs no rain in each grid box for the independent variable	Resultant rainfall occurrence over the past 30 min as determined by the cloud-top temperature field.
2	2	0 Min	In discriminant analysis the dependent variable can be modified as a means of varying the strength of the dependent variable	Precipitation occurrence over at least two stations will 1) help delineate between isolated showers and more significant rainfall events; 2) help eliminate undetected noise.
3	1	10 Min	Same as experiment 2.	Precipitation reaching the ground in association with various features of the cloud-top temperature field may occur approximately 10 min [Grifith (personal communication)] after the occurrence of these cloud-top variables. This delay may be due to intense updrafts (especially in the developing stage of a storm), strong surface winds and subcloud evaporation.
4	2	10 Min	Same as experiment 2.	Same as experiments 2 and 3.
5	1	30 Min	Same as experiment 2.	Detecting rainfall over the period following the recognition of convective cloud areas.
6	2	30 Min	Same as experiment 2.	Same as experiments 2 and 5.

independent data sets to test these models. The precipitation events on these days were all compatible with the type of convective systems targeted by the study. Selection of these days were based on the fact that each convective system was spread over a relatively large area and the rainfall sustained itself over an extended period. The constraints of pixel resolution, temporal frequency of the satellite data and the varying separation among surface stations made the study of small storms impractical.

a. Surface data

To verify the occurrence of rainfall, the CCOPE surface mesonet was used. The areal density of the CCOPE mesonet is comparable to mesonets in other locations where satellite rainfall studies have been conducted (e.g., Griffith et al., 1981). The surface mesonet consisted of 96 PROBE stations (Portable Remote OBservation of the Environment) and 27 PAM stations (Portable Automated Mesonet) arranged in a dense inner network and a sparse outer network as shown in Fig. 2. Spacing between the 71 PROBE stations within the outer network is approximately 20 km compared to 7 km for the 25 PROBE and 27 PAM stations making up the inner network. The PROBE and PAM stations measured rainfall accumulated over 5 and 1-min intervals, respectively. A thorough quality control analysis was done on both sets of data to eliminate anomalous rain reports.

To establish a statistical relationship between surface rainfall measurements and the cloud parameters, three different grids (each with a grid spacing of 20 km by 20 km) were overlayed onto portions of the surface mesonet as shown in Fig. 2. Each grid location served as an independent sample of rainfall verification. The grids used for the case study days 12 June, 13 July and 2 August generally fit the raingage density necessary to adequately observe rain areas of a cloud—reported by Silverman et al. (1981) to be 45–80 km^2 per gage. The grids for these days were overlayed onto the portion of the mesonet where the combination of PAM and PROBE station were most dense (July 13 used a somewhat different grid due to missing PAM data). Since rainfall on both 11 July and 1 August occurred over the sparse portion of the mesonet where surface stations were located 20 km apart, each grid contained only one surface station. Due to the lower density of surface

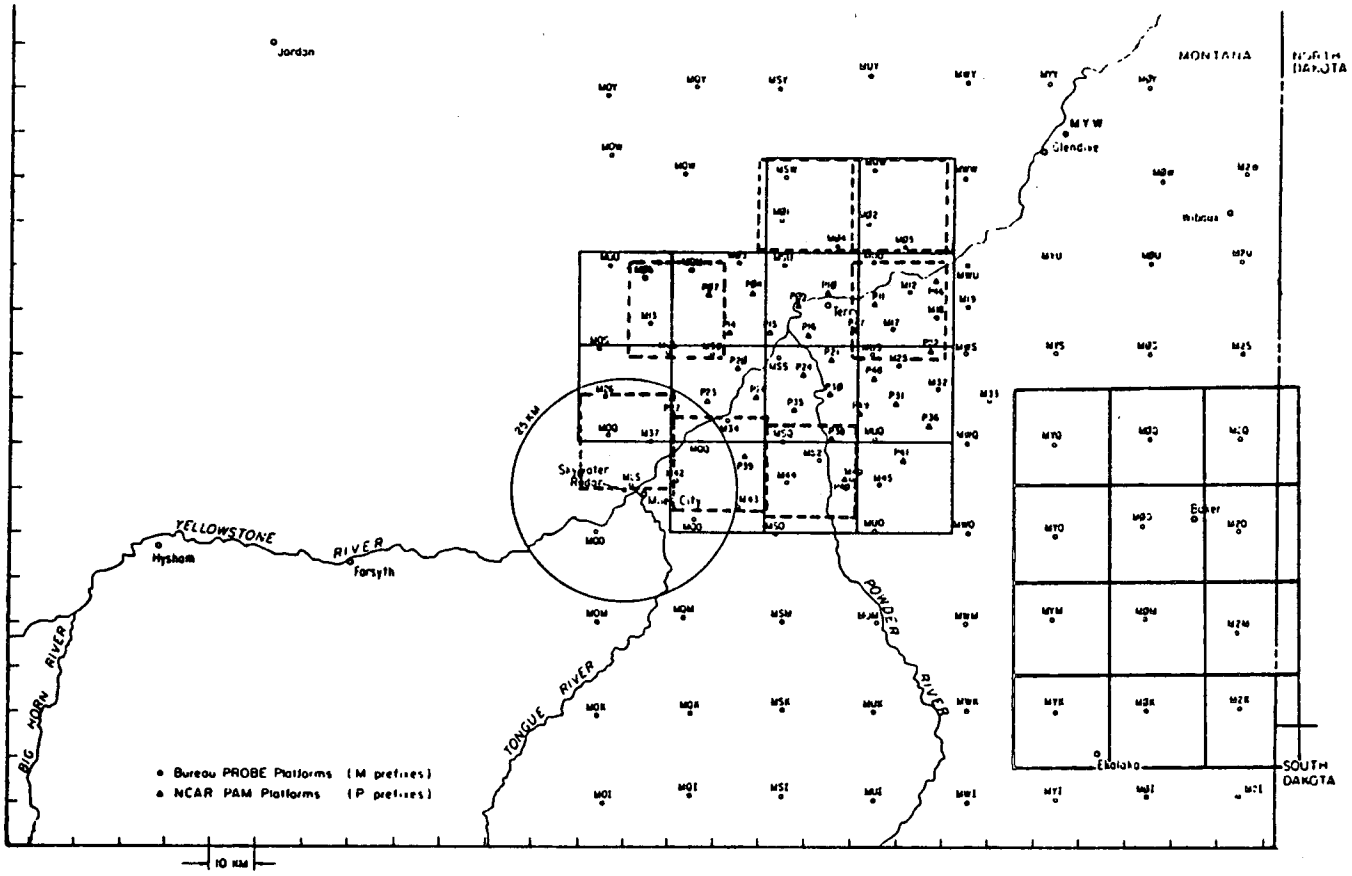

FIG. 2. The CCOPE surface meteorological data network with grid for initial data and 2 August storm no. 2 (solid lines); grid for 13 July (dashed line) on left; and grid for 11 July and 1 August (solid line) on right.

stations for the storm cases of 11 July and 1 August, these days were only used as test cases.

b. Satellite data

Infrared imagery were collected from the GOES-West satellite's Visible Infrared Spin Scan Radiometer (VISSR) at full resolution (8 km at satellite subpoint). For 12 June, 11 July and a portion of 13 July, the data were collected by Colorado State University's Direct Readout Satellite Earth station. The data for 1 and 2 August and the remainder of 13 July were collected at the University of Wisconsin's Space Science and Engineering Center. The latter data were obtained through the National Environmental Satellite Data and Information Service (NESDIS). Table 4 shows the dates and times of the satellite images processed for each case study day. Rainfall was classified over the 30-min time period between images with rainfall classifications carried out only for satellite images 30 min apart. From each of the satellite images, refined pixels of the cloud-top temperature field were obtained such that their size and location corresponded to the surface station grid.

Satellite data processing involved several steps necessary to properly orient the imagery over the surface mesonet. In any study comparing satellite data to surface rainfall, accurate navigation of the satellite data is essential. In this study, the satellite data were registered to an accuracy of one infrared pixel or less. Each image was then remapped to a Lambert Conformal map projection to geometrically orient the satellite data over the surface grid. Following this step the infrared radiance values were converted to their corresponding temperature values. The final step involved creating separate samples of infrared temperature corresponding to each surface grid box location. During this step an adjustment was made to the size and location correct for parallax (the displacement of a cloud from its actual location above the earth as seen by the satellite).

TABLE 4. Dates and times of GOES-West satellite images used in analysis.

Day (1981)	Number of images	Time of images (UTC)
12–13 June	8	0129, 0141, 0159, 0211, 0241, 0259, 0311, 0341
11–12 July	3	0205, 0235, 0305
13–14 July	8	0215, 0229, 0245, 0259, 0315, 0329, 0345, 0415
2–3 Aug. (storm no. 1)	6	2315, 2345, 0015, 0045, 0115, 0145
2–3 Aug. (storm no. 2)	5	0215, 0245, 0315, 0345, 0415

4. Cloud parameter analysis

In order to quantify how each cloud parameter is correlated to rainfall, and to estimate the magnitude by which each cloud parameter discriminates rainfall, each parameter was tested for all combinations of experiments and rain-rate thresholds using a box plot. A box plot is an alternative to a scatter plot when the dependent variable is coded into groups. Plotting was limited to those storm cases which were used to develop the statistical models. Table 5 quantifies the analysis performed on each cloud parameter by comparing the differences in the means. This table also denotes a code related to percentage overlap of the 95% confidence interval of the means for all samples verified at each rain-rate threshold. To provide a statistical measure of the reliability and consistency of these results, the medians of the 5 and 20% largest values of each cloud parameter were calculated and analyzed. Neither of the statistically smoothed versions of each cloud parameter showed a distinctive difference in the degree of correlation to rainfall.

The parameters most correlated to rainfall in the colder more convective cloud regions were CCTT, DEL-CCTT, AVGCCT, CTSTT, DEL-AVGCCT, CGRAD, CLAP, CGRADT and CLAPDT. The best discrimination is associated with both the higher rain-rate thresholds and the 10-min delayed rainfall verification. Although decreasing cloud-top temperatures are highly correlated with rainfall occurrence, the parameters DEL-GRAD, DEL-CGRAD, DEL-LAP, DEL-CLAPDT and DEL-CGRADT all showed that decreases of potentially convective cloud regions may also correlate with rainfall. The implication is that the coldest cloud-top temperature may continue to decrease even though other indicators of localized convection have begun to diminish. The cloud parameters LAP and DEL-CLAP exhibited such random patterns that they were not considered reliable for model selection.

5. Results and analysis

Results from the best statistical models for each experiment and rain rate are given in Tables 6 and 7. The total number of samples used were 166[1] from the initial data and 144[2] from the test data. Since experiments 2, 4, and 6 were devised to verify the results of experiments 1, 3, and 5, the main emphasis of discussion will focus on experiments 1, 3, and 5.

[1] One sample was an extreme outlier, caused by a localized heavy shower from a small secondary cell. This sample was dropped from the rain rate experiments in which it was determined to be overly influential.

[2] Missing surface data in experiment 3 resulted in three less samples.

TABLE 5. Cloud parameters for all experiments and rain-rate thresholds comparing the mean of rainfall and no-rainfall samples and percentage of overlap for a 95% confidence interval of the means where, asterisk equals no overlap, plus equals less than 25% overlap, pound sign equals 25 to 50% overlap, and minus equals greater than 50% overlap.

		Expt. no. 1		Expt. no. 2		Expt. no. 3		Expt. no. 4		Expt. no. 5		Expt. no. 6	
CCTT	1.0	−2.63	+	−2.27	#	−3.00	+	−3.98	*	−6.02	*	−5.30	*
	4.0	−5.61	*	−6.93	*	−6.33	*	−7.72	*	−6.73	*	−7.73	*
	10.0	−4.98	*			−6.30	*			−6.53	*		
GRAD	1.0	0.17	−	0.15	−	0.26	−	0.28	−	−0.35	−	−0.55	−
	4.0	−0.49	−	−0.43	−	−0.23	−	−0.13	−	−0.31	−	−0.41	−
	10.0	−0.20	−			−0.07	−			0.11	−		
CGRAD	1.0	0.19	−	0.01	−	0.31	−	0.19	−	0.03	−	−0.12	−
	4.0	−0.04	−	0.16	−	0.10	−	0.24	−	0.10	−	−0.10	−
	10.0	0.22	−			0.36	−			0.24	−		
LAP	1.0	0.56	−	0.57	−	0.81	−	0.28	−	−0.47	−	−0.90	#
	4.0	−0.58	−	−0.26	−	0.08	−	0.35	−	−0.09	−	−0.17	−
	10.0	0.001	−			0.60	−			0.65	−		
CLAP	1.0	0.66	−	0.52	−	0.81	−	0.68	−	0.17	−	0.02	−
	4.0	0.37	−	0.99	−	0.50	−	1.11	−	0.31	−	−0.11	−
	10.0	0.71	−			0.93	−			0.64	−		
AVGCCT	1.0	−1.28	−	−1.45	−	−1.37	−	−2.95	#	−5.36	*	−5.39	*
	4.0	−5.42	*	−6.86	*	−5.48	*	−7.64	*	−6.69	*	−8.57	*
	10.0	−4.08	+			−5.58	*			−6.25	*		
CTSTT	1.0	−4.52	*	−4.06	*	−4.19	*	−5.63	*	−7.48	*	−7.04	*
	4.0	−6.89	*	−8.79	*	−7.00	*	−8.83	*	−7.74	*	−9.38	*
	10.0	−5.72	*			−6.71	*			−6.59	*		
CLAPDT	1.0	−0.008	−	−0.007	−	−0.010	−	−0.006	−	0.005	−	0.007	−
	4.0	0.002	−	−0.009	−	0.004	−	−0.010	−	0.003	−	0.012	−
	10.0	−0.005	−			−0.005	−			−0.003	−		
CGRADT	1.0	−0.001	−	0.003	−	−0.003	−	0.001	−	0.005	−	0.007	#
	4.0	0.006	−	0.002	−	0.002	−	0.002	−	0.004	−	0.008	+
	10.0	0.001	−			0.001	−			0.001	−		
DEL-CCTT	1.0	−2.13	#	−2.16	#	−0.08	−	−0.95	−	4.31	*	3.43	+
	4.0	0.67	−	0.72	−	2.56	#	2.75	#	5.62	*	6.99	*
	10.0	−0.07	−			2.54	#			6.12	*		
DEL-GRAD	1.0	−0.47	−	−1.03	−	−0.49	−	−0.31	−	−0.046	−	0.24	−
	4.0	0.32	−	0.37	−	0.26	−	0.16	−	0.69	−	0.53	−
	10.0	0.33	−			0.70	#			−0.04	−		
DEL-CGRAD	1.0	0.005	−	0.22	−	−0.21	−	−0.20	−	−0.06	−	−0.04	−
	4.0	0.28	−	0.12	−	0.17	−	0.002	−	0.005	−	0.37	−
	10.0	−0.14	−			0.04				−0.07	−		
DEL-LAP	1.0	−1.00	−	−0.76	−	−1.13	#	−0.56	−	−0.14	−	0.28	−
	4.0	0.62	−	0.19	−	0.17	−	0.01	−	0.59	−	0.13	−
	10.0	0.64	−			−0.12	−			−0.21	−		
DEL-CLAP	1.0	−0.15	−	−0.12	−	−0.42	−	−0.56	−	−0.06	−	−0.04	−
	4.0	0.22	−	−0.40	−	0.07	−	−0.48	−	−0.14	−	0.50	−
	10.0	0.09	−			−0.23	−			−0.56	−		
DEL-AVGCCT	1.0	−2.96	+	−2.46	#	−2.49	#	−0.48	−	2.49	#	3.05	+
	4.0	0.86	−	0.77	−	2.02	#	2.97	#	5.16	*	7.00	*
	10.0	−0.20	−			2.25	#			5.32	*		
DEL-CLARDT	1.0	0.001	−	−0.003	−	0.006	−	0.007	−	−0.007	−	−0.006	−
	4.0	−0.008	−	0.005	−	−0.008	−	0.004	−	−0.006	−	−0.014	#
	10.0	−0.005	−			−0.001	−			0.001	−		
DEL-CGRADT	1.0	−0.001	−	−0.010	−	0.003	−	−0.002	−	−0.004	−	−0.005	−
	4.0	0.025	−	−0.004	−	−0.007	−	−0.003	−	−0.007	−	−0.008	+
	10.0	−0.005	−			−0.004	−			−0.005	−		

TABLE 6. The percentage and number of correctly classified samples for both the initial and test data sets for all rain-rate thresholds for experiments 1, 3, and 5. The subscripts of the cloud parameters (from Table 2) for each tested statistical model are listed in order of parameter significance.

Observed samples for each data set		Classified samples for Experiment #1			Classified samples for Experiment #3			Classified samples for Experiment #5		
		Percent correct	No rain	Rain	Percent correct	No rain	Rain	Percent correct	No rain	Rain
Initial data	No rain	66.2	51	26	66.7	54	27	62.5	50	30
	Rain	82.0	16	73	69.4	26	59	81.2	16	69
August 2 storm #2	No rain	8.9	3	31	47.2	17	19	17.1	6	29
	Rain	100.0	0	31	89.7	3	26	96.7	1	29
August 1	No rain	29.6	16	38	51.9	27	25	40.4	21	31
	Rain	100.0	0	18	85.0	3	17	94.1	1	16
July 12	No rain	0.0	0	2	0.0	0	5	11.1	1	8
	Rain	37.5	3	5	100.0	0	5	100.0	0	1
		Rain rate cutoff = 1.0 mm h^{-1}			Rain rate cutoff = 1.0 mm h^{-1}			Rain rate cutoff = 1.0 mm h^{-1}		
Statistical model		10, 6, 1, 7, 18			1, 6, 10, 3			1, 15, 10, 11		
Initial data	No rain	82.5	99	21	83.1	98	20	81.5	101	23
	Rain	71.1	13	32	68.1	15	32	57.1	18	24
August 2 storm #2	No rain	34.9	15	28	60.0	27	18	54.3	25	21
	Rain	100.0	0	22	90.0	2	18	95.5	1	18
August 1	No rain	72.9	43	16	84.5	49	9	75.4	43	14
	Rain	84.6	2	11	85.7	2	12	91.6	1	11
July 12	No rain	25.0	1	3	14.3	1	6	22.2	2	7
	Rain	100.0	0	6	100.0	0	3	0.0	1	0
		Rain rate cutoff = 4.0 mm h^{-1}			Rain rate cutoff = 4.0 mm h^{-1}			Rain rate cutoff = 4.0 mm h^{-1}		
Statistical model		1, 15, 13			1, 15, 11, 7			1, 11, 9		
Initial data	No rain	85.5	112	19	81.8	108	24	88.1	119	16
	Rain	61.8	13	21	61.8	13	21	48.4	16	15
August 2 storm #2	No rain	55.5	31	25	63.0	34	20	84.2	48	9
	Rain	100.0	0	9	100.0	0	11	37.5	5	3
August 1	No rain	85.7	54	9	92.1	58	5	83.6	51	10
	Rain	88.8	1	8	88.8	1	8	60.0	3	5
July 12	No rain	12.5	1	7	10.0	1	9	10.0	1	9
	Rain	100.0	0	2						
		Rain rate cutoff = 10.0 mm h^{-1}			Rain rate cutoff = 10.0 mm h^{-1}			Rain rate cutoff = 10.0 mm h^{-1}		
Statistical model		15, 1, 11, 7			1, 15, 11, 7			11, 2, 10, 6, 15, 7		

a. Statistical model overview

The most noteworthy results were achieved in experiment 1 at the 10 mm h^{-1} rain-rate threshold and in experiment 3 at the 4 and 10 mm h^{-1} rain-rate thresholds. The cloud parameters selected for these statistical models are very similar. The parameters CCTT and DEL-AVGCCT were the most significant classifiers of these models followed by DEL-GRAD and CTSTT. AVGCCT was the strongest cloud parameter for experiments 2 and 4. Results from the 4 mm h^{-1} rain-rate case in experiment 5 are consistent with results for experiment 3 at the 4 and 10 mm h^{-1} rain rates in both percentage of correctly classified samples and of the two cloud parameters (CCTT and DEL-GRAD) selected for the statistical models. The parameters CCTT, DEL-CCTT, AVGCCT and DEL-AVGCCT were the most common classifiers for the 1 mm h^{-1} rain-rate threshold. The parameters CCTT, AVGCCT and DEL-AVGCCT are the most important classifiers overall.

TABLE 7. As in Table 6 for experiments 2, 4 and 6.

Observed samples for each data set		Classified samples for experiment no. 2			Classified samples for experiment no. 4			Classified samples for experiment no. 6		
		Percent correct	No rain	Rain	Percent correct	No rain	Rain	Percent correct	No rain	Rain
Initial data	No rain	65.8	73	38	60.0	66	44	49.6	57	58
	Rain	78.2	12	43	67.9	18	38	76.0	12	38
2 August storm no. 2	No rain	31.8	14	30	34.1	15	24	4.4	2	43
	Rain	90.5	2	19	95.2	1	20	100.0	0	20
		Rain rate cutoff = 1.0 mm h^{-1}			Rain rate cutoff = 1.0 mm h^{-1}			Rain rate cutoff = 1.0 mm h^{-1}		
Statistical model		15, 7, 5, 9, 17			15, 8, 5, 1			7		
Initial data	No rain	88.2	127	17	85.8	121	20	89.0	129	16
	Rain	77.3	5	17	70.8	7	17	57.1	9	12
2 August storm no. 2	No rain	65.5	36	19	82.7	43	9	73.7	42	15
	Rain	80.0	2	8	69.2	4	9	75.0	2	6
		Rain rate cutoff = 4.0 mm h^{-1}			Rain rate cutoff = 4.0 mm h^{-1}			Rain rate cutoff = 4.0 mm h^{-1}		
Statistical model		6, 15, 5, 11, 8			6, 5, 10, 8			6, 2, 12		

b. Analysis of experiments

Plots of the percentages of correctly classified rain and no-rain samples appear in Fig. 3. Consistently high percentages of correctly classified rainfall samples were obtained for all rain-rate thresholds in experiments 1 and 3. The best results were found in experiment 3, in which the period of rainfall verification was moved forward by 10 min. This adjustment makes the instantaneous properties of the cloud-top temperature field more representative of surface rainfall. A 10-min time lag when combined with a 10 mm h^{-1} rain-rate threshold offers the best overall discrimination of rain and no-rain samples; success rates are over 60%. These latter results are particularly important because they mean that heavier rain episodes can be identified with statistically significant accuracy, regardless of the fact that their frequency of occurrence is low.

Poor no-rain classification for the 11 July case may be attributed to both lower raingage density and the convective system's rapid development at the time of study. Since the storm cases used in the initial data set were not undergoing such rapid development, the derived models may not have correlated well with this storm case. As a consequence, results from the 11 July case will not be incorporated into further discussion of the results.

The 1 August storm case does not seem affected by the lower density of raingages; results are consistent with the test case of 2 August Storm No. 2. With the exception of 11 July, the percentage of correctly classified light rain and no-rain samples at the 10 mm h^{-1} threshold is greater than 50% for all three experiments. This demonstrates that significant improvement in filtering out light rain and no-rain samples is easily obtained by raising the rain-rate threshold.

Differences in the level of convective activity appear to support the higher accuracy of rainfall classification among the test dataset. Overall convective activity was more intense for the case study days of 1 August and both storms of 2 August compared to 12 June and 13 July. As a result, such cloud parameters as CCTT and DEL-AVGCCT correlate more closely with the test cases than with the combination of cases within the initial data set. Percentages of correctly classified rain samples for experiment 5 appear less stable than in experiment 1 and 3. Lower percentages of correctly classified rain samples at the 10 mm h^{-1} rain-rate threshold may be attributed to either new convective development or the advance of new rain areas.

Experiments 2, 4, and 6 were included as a more absolute measure of rainfall verification at the surface. In these experiments as least two surface stations were required to verify rainfall. Although these later experiments may erroneously smooth or eliminate some rainfall events, they do help to verify the accuracy and consistency of experiments 1, 3 and 5. Raising the rain rate cutoff to 4 mm h^{-1} increased the accuracy of no-rain classification with a corresponding small decrease for rain classification. Though the success rates do not match exactly with experiments 1, 3 and 5, there is overall consistency between the two sets of experiments.

6. Summary and conclusions

This study used a statistical discriminant analysis technique to identify intense rainfall regions occurring

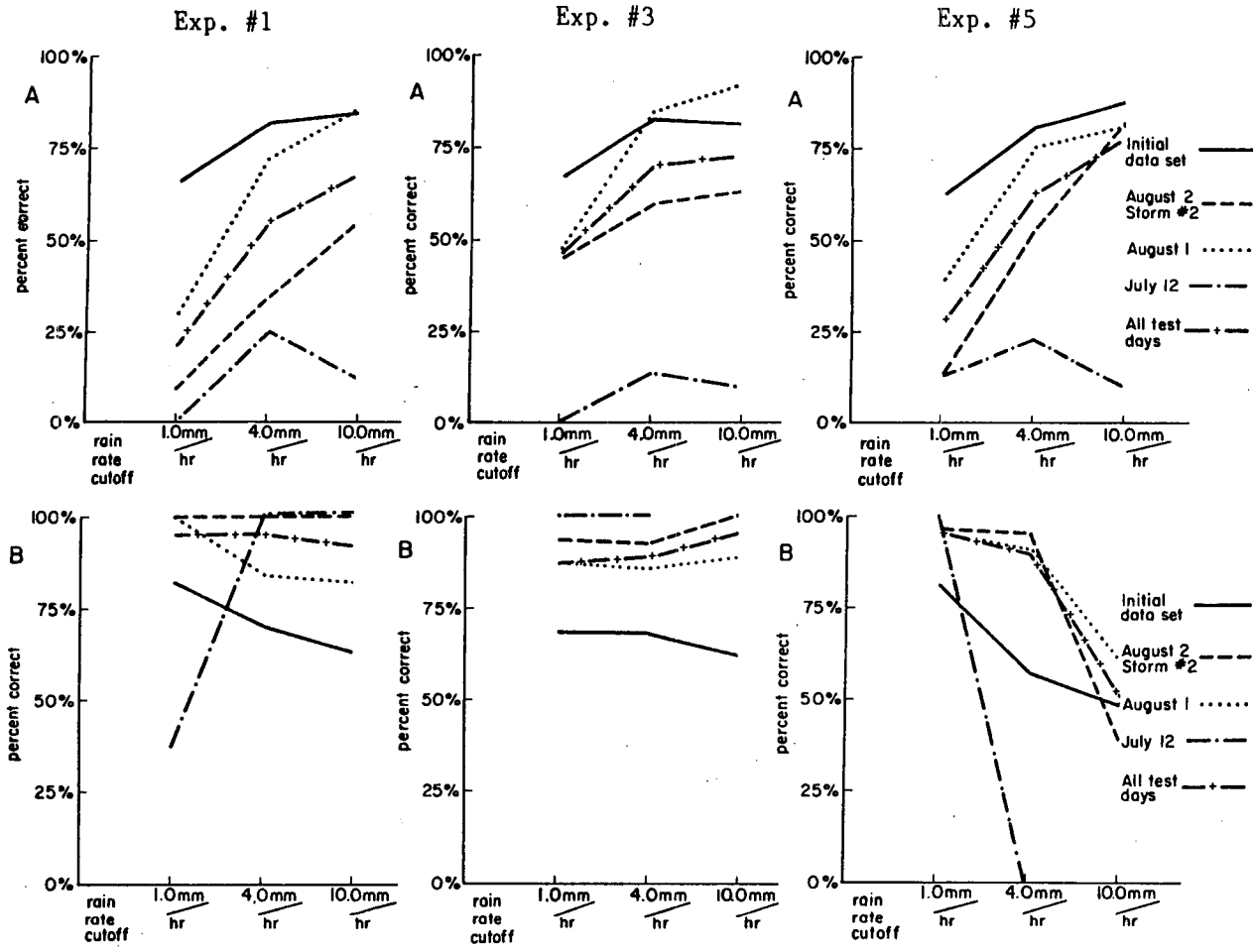

FIG. 3. The percentage of samples correctly classified as no-rain and/or rain below each rain rate threshold (A) and rainfall at or above each rain rate threshold (B) for the best statistical models derived from experiments 1, 3 and 5.

at low frequency from higher frequency light and no-rainfall regions occuring within large convective cloud systems over the United States High Plains. Parameters derived from the GOES-West infrared cloud-top temperature field were used as the discriminator variables. The convective systems under analysis occurred during the CCOPE field project, held near Miles City, Montana in the summer of 1981.

As illustrated in Fig. 1, observed rainfall rates of 10 mm h^{-1} or more contributed to 75% of the total volumetric rainfall within the CCOPE domain. This study has demonstrated skill in classifying these significant rain events by successfully filtering out many of the light and no-rain events. Overall performance of the discriminant technique increased as the rain-rate threshold was raised from 1 to 4 mm h^{-1} and finally to 10 mm h^{-1}. The highest success rates (>60%) of correctly classified samples is achieved when the 30-min window of rainfall verification is lagged by 10 min at the 4 and 10 mm h^{-1} rain-rate thresholds. Success rates of 50% and higher are achieved using 0 and 30-min time lags at either the 4 and 10 mm h^{-1} rain-rate thresholds.

The evidence indicates that the incorporation of a 10-min time delay more realistically relates certain features of the cloud-top temperature field with precipitation occurrence on the ground. Light rain events were not easily distinguishable from no-rain events, suggesting that light rainfall may occur too randomly within the cloud to be adequately classified. The coldest cloud-top temperature, spatially averaged cloud-top temperature, and the change over time of average cloud-top temperature, were found to be the best parameters for rainfall classification in this study. These parameters are most highly correlated with the regions of convection in organized convective systems over the CCOPE domain.

Comparing these results with other studies confirm that certain parameters outperform others in detecting rainfall. Adler et al. (1985) used the correlation of minimum cloud top temperature, its difference from the tropopause temperature, and their respective change

over time in detecting severe storms which are generally associated with higher rain rates. The areal extent of cold cloud and its variation with time as measured by the average cloud-top temperature have been shown by Griffith et al. (1978) to provide reasonable estimates of total volumetric rainfall. The maximum Laplacian of the cloud-top temperature did not significantly improve rainfall detection in either Whitney (1982) or this study. The tightest gradient of the cloud-top temperature helped increase rainfall detection in both this study and Whitney (1982), but all parameters related to gradient never surpass the correlation associated with minimum cloud-top temperature.

The importance of identifying significant rain areas in convective systems is clearly evident based on the dominance of the heavy rain systems to the total volumetric rainfall. This factor is of particular relevance over the United States High Plains, where high cloud bases as well as significant subcloud evaporation reduces the frequency of heavy rainfall events. However, although cloud top temperature parameters demonstrate skill in classifying significant rainfall events, there are limits to how much further accuracy can be obtained using infrared data exclusively. Increased spatial resolution would clearly improve the interpretation of cloud-top temperature structure: however, an alternate approach would consider an additional channel sensitive to cloud liquid water.

Acknowledgments. The authors acknowledge Thomas H. Vonder Haar for his suggestions during the course of this research at Colorado State University. Appreciation is extended to Research and Data Systems Corporation and also Ms. Anna Nelson of The Florida State University, Department of Meteorology, for their help in preparing the manuscript. This investigation was supported by the National Oceanic and Atmospheric Administration under Contract NA81AA-0-00058.

REFERENCES

Adler, R. F., M. J. Markus and D. D. Fenn, 1985: Detection of severe Midwest thunderstorms using geosynchronous satellite data. *Mon. Wea. Rev.*, **113,** 769–781.

Arkin, P. A., 1979: The relationship between fractional coverage of high cloud and rainfall accumulations during GATE over the B-scale array. *Mon. Wea. Rev.*, **107,** 1382–1387.

Augustine, J. A., 1984: The diurnal variation of large-scale infrared rainfall over the tropical Pacific Ocean during August 1979. *Mon. Wea. Rev.*, **112,** 1745–1751.

Changnon, S. A., 1975: A High Plains climatography. Illinois State Water Survey, Urbana, IL, 119 p.

DelBeato, R., and S. L. Barrell, 1985: Rain estimation in extratropical cyclones using GMS imagery. *Mon. Wea. Rev.*, **113,** 747–755.

Dixon, W. J., M. B. Brown, L. Engelman, J. W. Frane, M. A. Hill, R. I. Jennrich and J. D. Toparek, 1983: *BMDP Statistical Software.* University of California Press,

Doneaud, A. A., S. Ionescu-Niscov and J. R. Miller, 1984a: Convective rain-rates and their evolution during storms in a semi-arid climate *Mon. Wea. Rev.*, **112,** 1602–1612.

——, ——, D. L. Priegnitz and D. L. Smith, 1984b: The area-time integral as an indicator for convective rain volumes. *J. Climate Appl. Meteor.*, **23,** 555–561.

Griffith, C. G., W. L. Woodley, P. G. Grube, D. W. Martin, J. Stout and D. N. Sikdar, 1978: Rain estimation from geosynchronous satellite imagery—visible and infrared studies. *Mon. Wea. Rev.*, **106,** 1153–1171.

——, J. A. Augestine and W. L. Woodley, 1981: Satellite rain estimation in the U.S. High Plains. *J. Appl. Meteor.*, **20,** 53–66.

Lovejoy, S., and G. L. Austin, 1979a: The delineation of rain areas from visible and IR satellite data for GATE and Mid-Latitudes. *Atmos. Ocean,* **20,** 77–92.

——, and ——, 1979b: The source of error in rain amount estimating schemes from GOES visible and IR satellite data. *Mon. Wea. Rev.*, **107,** 1048–1054.

Moses, J. F., 1984: Applications of automatic cloud detectors to interactive meteorological operations. *Preprints, Conf. on Satellite Remote Sensing and Applications,* Amer. Meteor. Soc., 178–184.

Negri, A. J., R. F. Adler and P. J. Wetzel, 1984: Rain estimation from satellites: an examination of the Griffith-Woodley technique. *J. Climate Appl. Meteor.*, **23,** 102–116.

Reynolds, D. N., and E. A. Smith, 1979: Detailed analysis of composited digital radar and satellite data. *Bull. Amer. Meteor. Soc.*, **60,** 1024–1037.

Scofield, R. A., and V. J. Oliver, 1977: A scheme for estimating convective rainfall from satellite imagery. NOAA Tech. Memo. NESS 86, NOAA-NESS, 47 p.

Silverman, B. A., L. K. Rogers and D. Dahl, 1981: On the sampling variance of raingage networks. *J. Appl. Meteor.*, **20,** 1468–1478.

Stout, J. E., D. W. Martin and D. H. Sikdar, 1979: Estimating GATE rainfall with geosynchronous satellite images. *Mon. Wea. Rev.*, **107,** 585–598.

Weisberg, S., 1980: *Applied Linear Regression.* John Wiley and Sons, 283 p.

Whitney, L. F., 1982: A statistical approach to rainfall estimation using satellite and conventional data. NOAA Tech. Rep. NESS. 89, NOAA-NESS, 50 p.

Wylie, D. P., 1979: An application of a geostationary satellite rain estimation technique to an extratropical area. *J. Appl. Meteor.*, **18,** 1640–1648.